Electronic Supplementary Material (ESI) for Energy & Environmental Science.

Supporting Information

15.8% Efficiency Binary All-Small-Molecule Organic Solar Cells Enabled by a Selenophene substituted Sematic Liquid Crystalline Donor

Tongle Xu[1,2,†], Jie Lv[1,2, †], Ke Yang[1, †], ZongYu Sun[1,2], Ya He[3], Qianguang Yang [1,2], Haiyan Chen[1], Qianqian Chen[1,2], Zhihui Liao[1,2], Zhipeng Kan[1], Tainan Duan[1], Kuan Sun[4], Jianyong Ouyang[3], Shirong Lu[1,*]

[1]Chongqing Institute of Green and Intelligent Technology, Chongqing School, University of Chinese Academy of Sciences (UCAS Chongqing), Chinese Academy of Sciences, Chongqing 400714, P. R. China.

[2]University of Chinese Academy of Sciences, Beijing 100049, P. R. China.

[3]Department of Materials Science and Engineering, National University of Singapore, 7 Engineering Drive 1, Singapore 117574, Singapore

[4]School of Energy & Power Engineering, MOE Key Laboratory of Low-Grade Energy Utilization Technologies and Systems, CQU-NUS Renewable Energy Materials & Devices Joint Laboratory, Chongqing University, Chongqing 400044, China

[†]These authors contributed equally: Tongle Xu, Jie Lv, Ke Yang

*Email: lushirong@cigit.ac.cn

Contents

Supplementary Figures

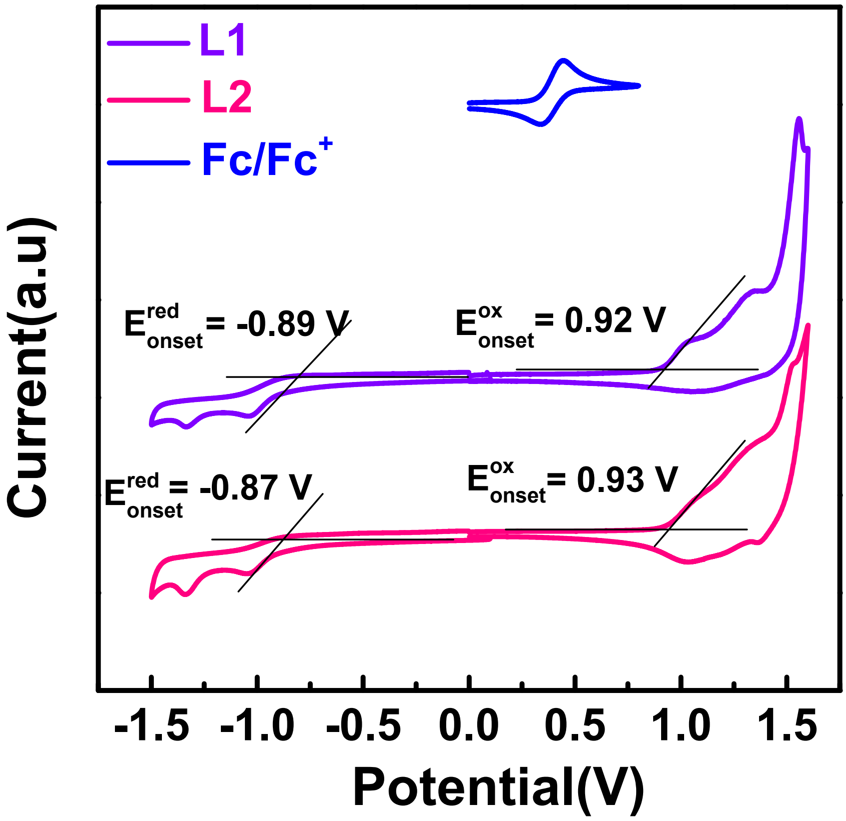

Figure S1. Cyclic voltammograms (CV) of L1, L2 and Fc/Fc^+ in 0.1 mol·L^{-1} tetrabutylammonium hexafluorophosphate (Bu_4NPF_6) acetonitrile solution.

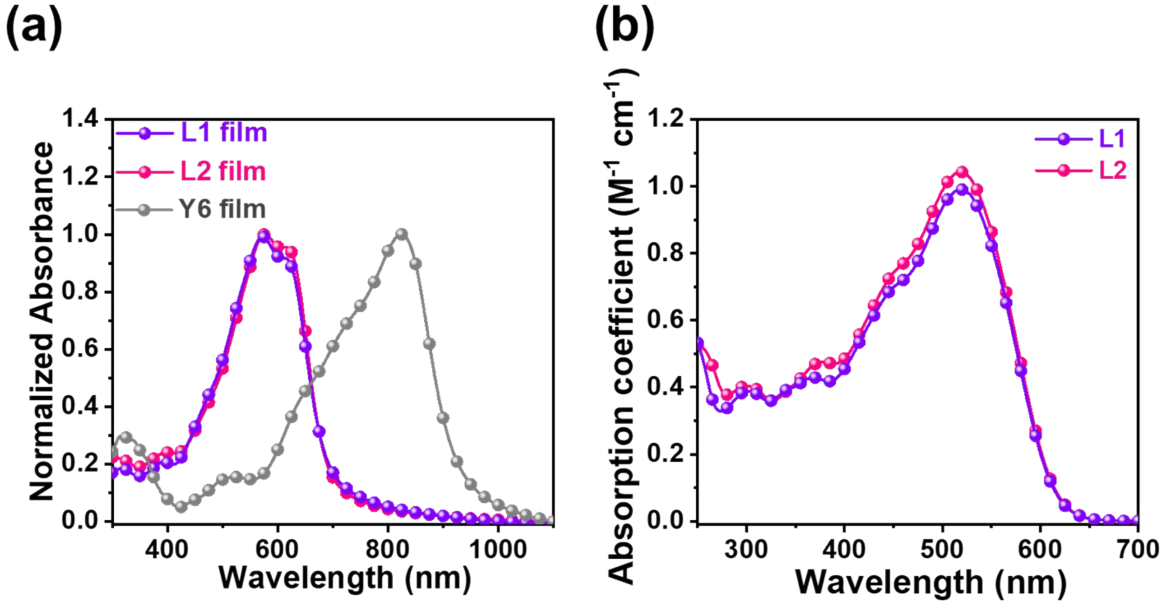

Figure S2. (a) Normalized film absorption spectra of L1, L2 and Y6, (b) the molar extinction coefficient profiles of L1 and L2 in chloroform.

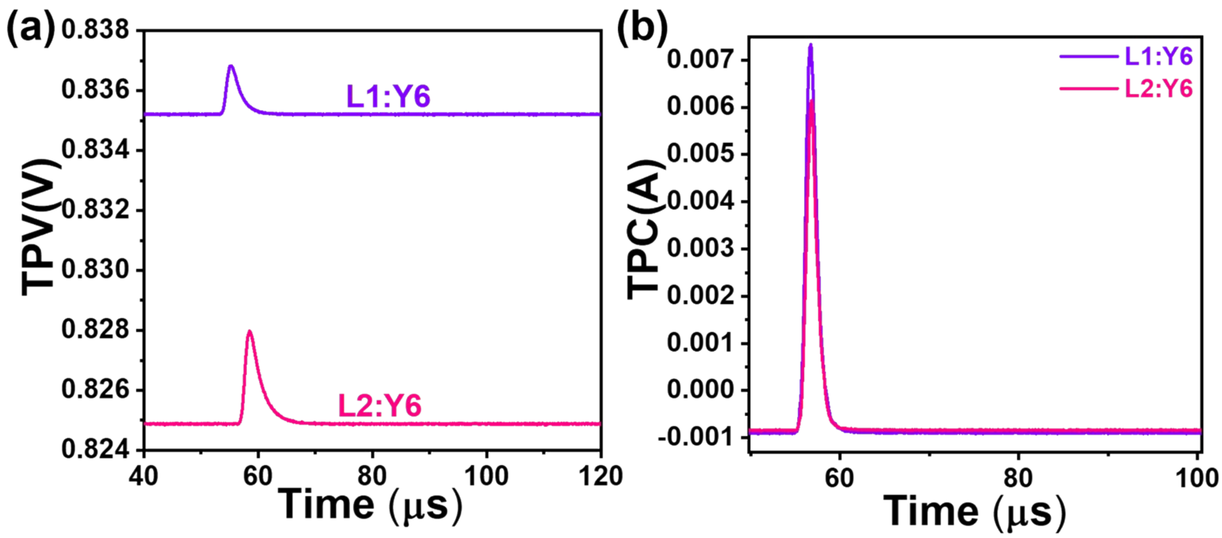

Figure S3. (a) Transient photovoltage (TPV) and (b) transient photocurrent (TPC) measurements of L1:Y6 and L2:Y6 based devices.

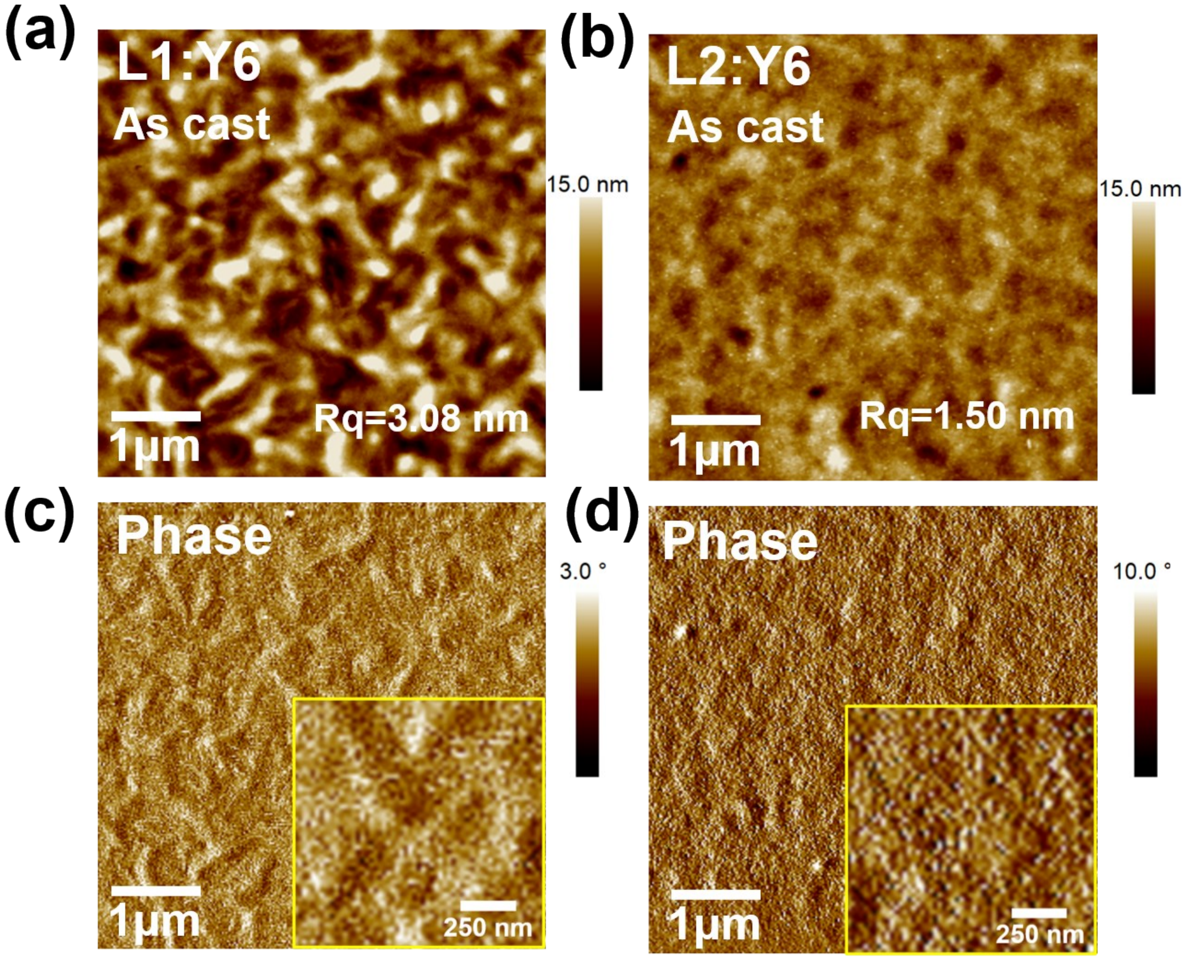

Figure S4. AFM height images (a, b) and AFM phase images (c, d) of L1:Y6 and L2:Y6 "as cast" blend films.

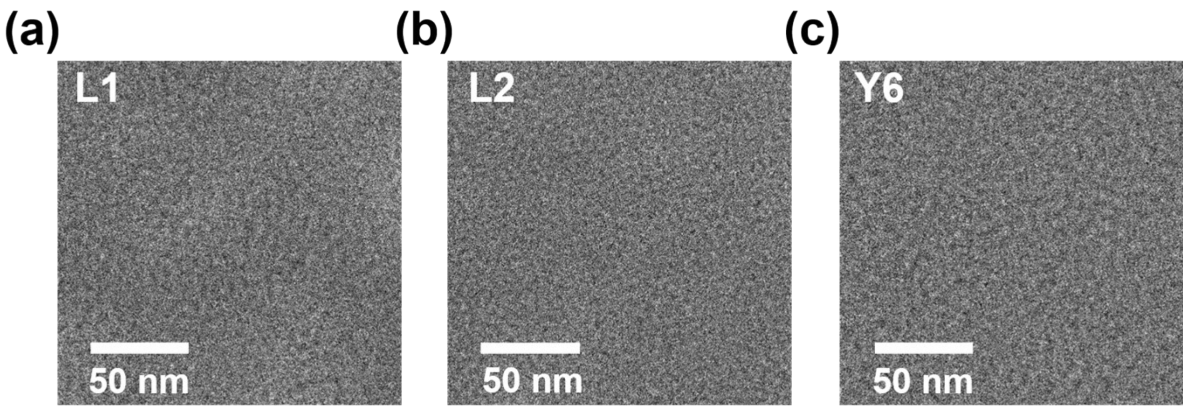

Figure S5. TEM images of L1, L2 and Y6 pure film**.**

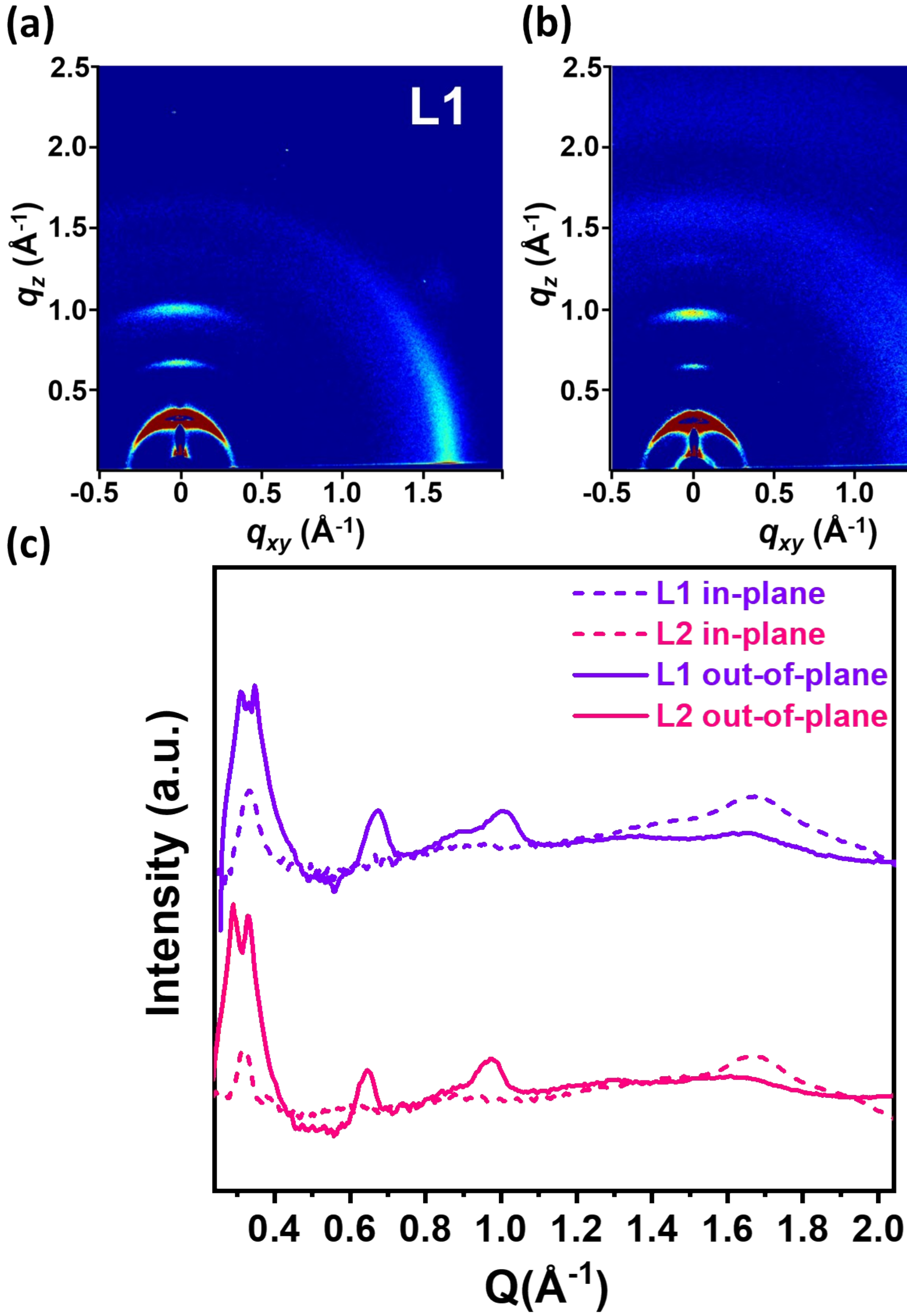

Figure S6. GIWAXS two-dimensional diffraction patterns of (a) L1, (b) L2 neat films; (c) corresponding in-plane (the dot lines) and out-of-plane (the solid lines) line-cut profiles.

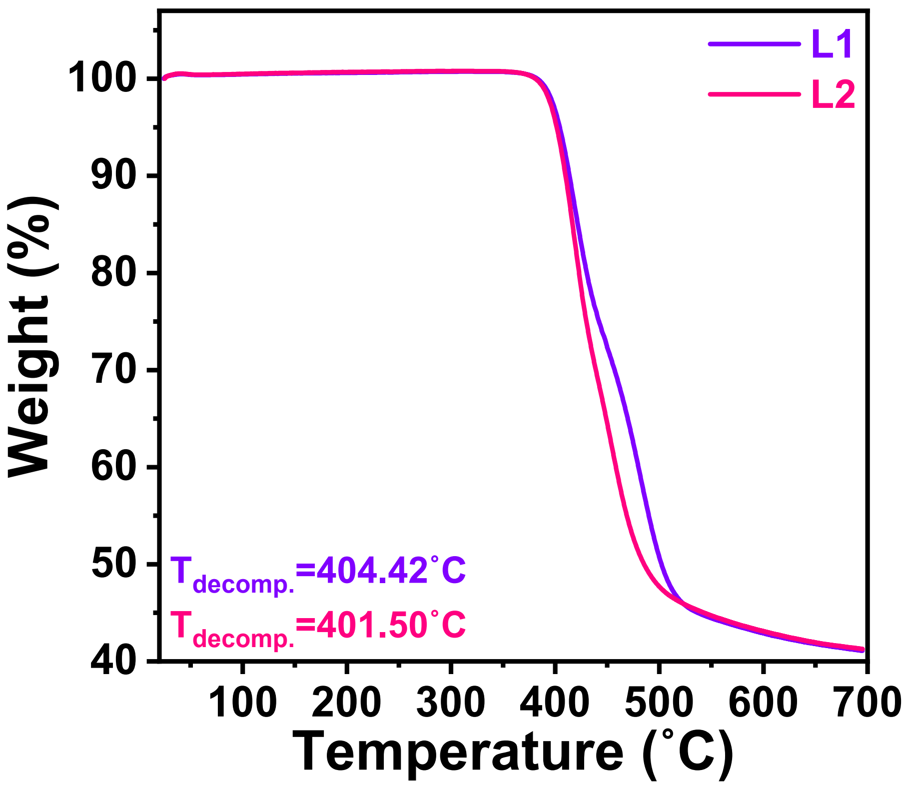

Figure S7. Thermogravimetric analysis (TGA) curve of the L1 and L2 with a heating rate of 10 °C/min under nitrogen atmosphere.

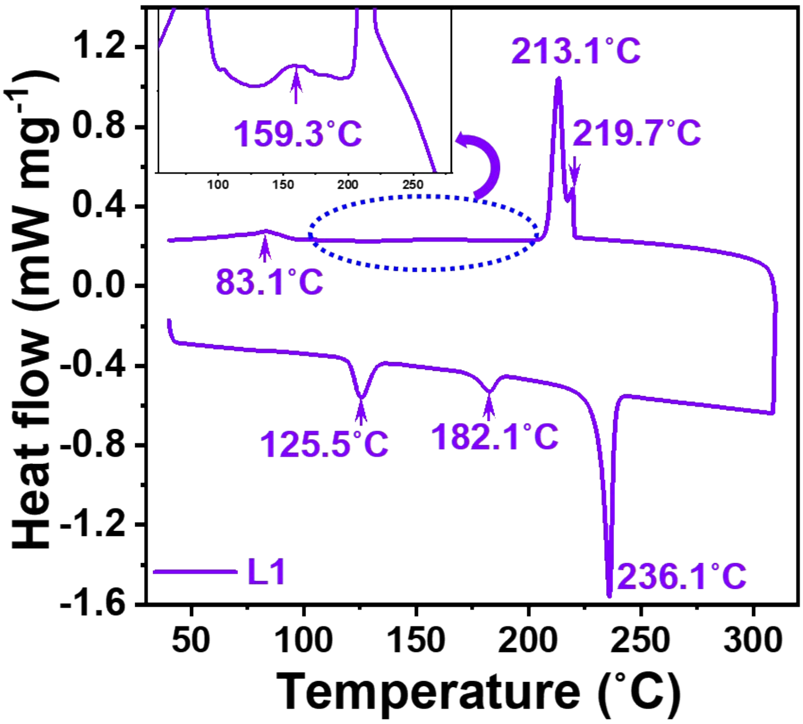

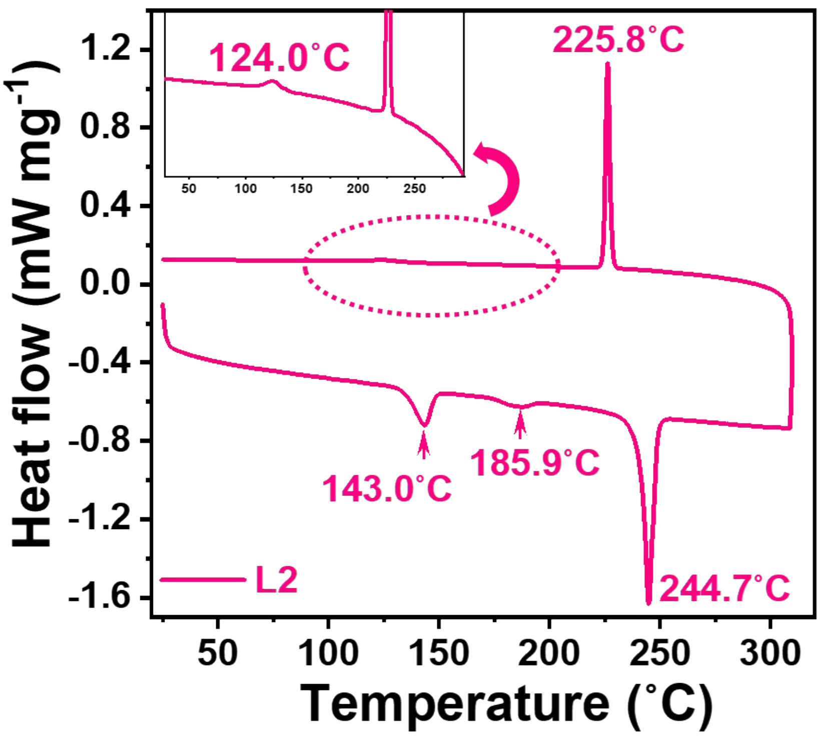

Figure S8. DSC traces of L1 and L2 with heating and cooling 10 ℃/min under nitrogen atmosphere.

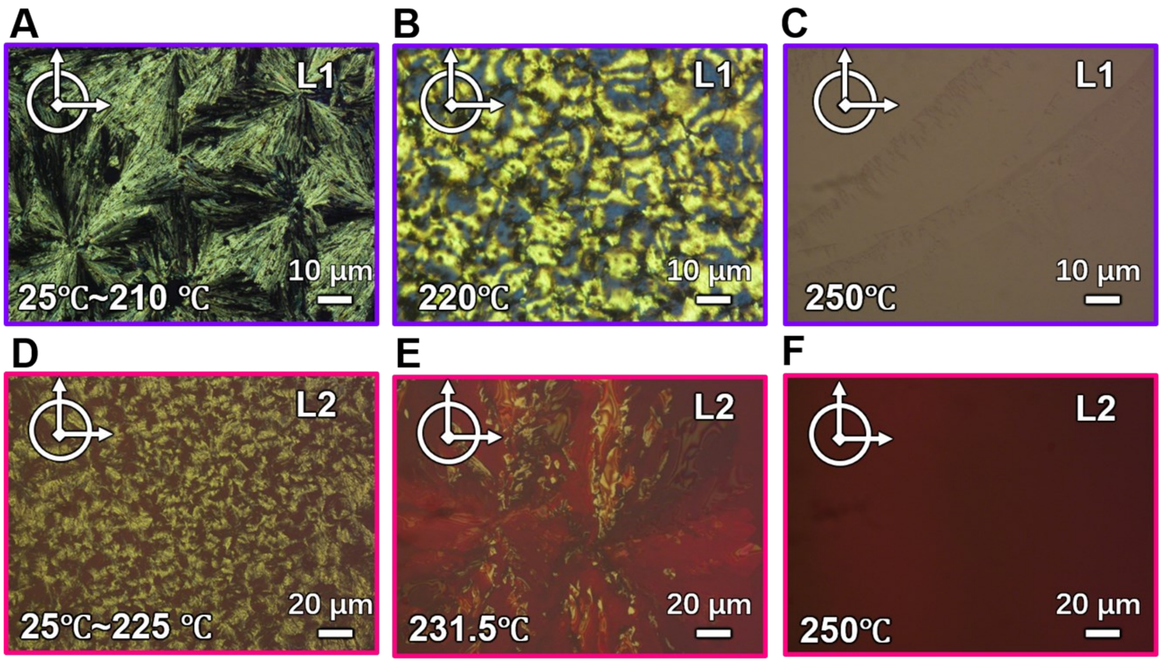

Figure S9. POM images of L1 and L2 neat films taken at different temperature. The angle of the polarizer and the analyzer is 90°.

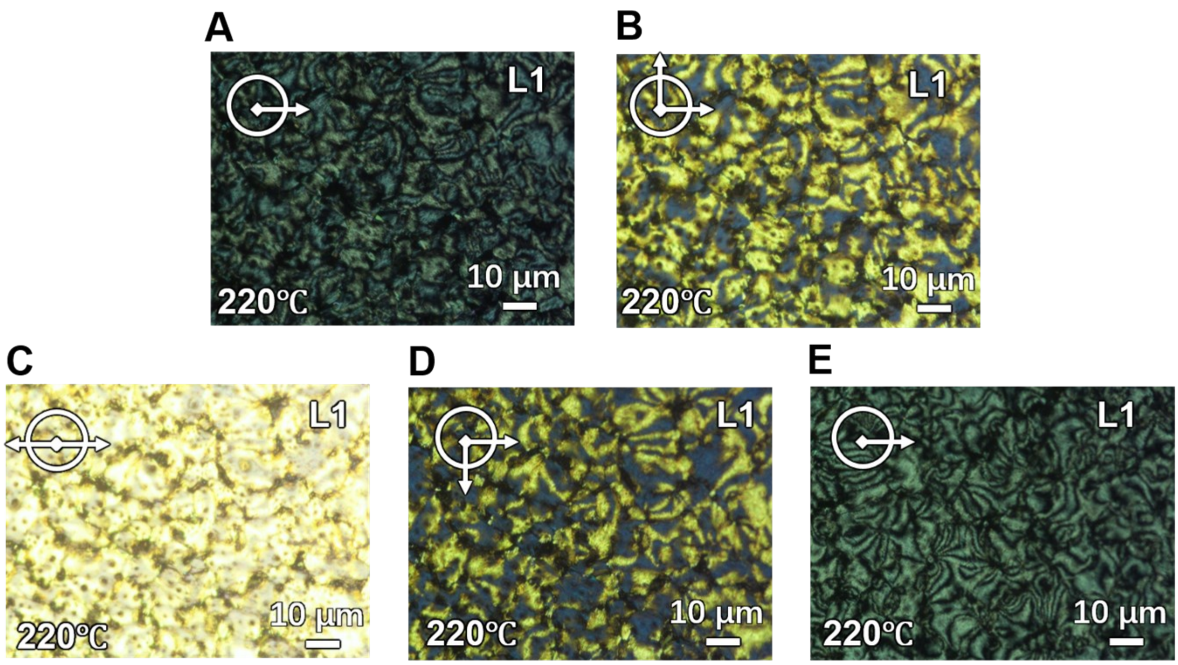

Figure S10. POM images of L1 neat film taken at different polarizer and the analyzer angles.

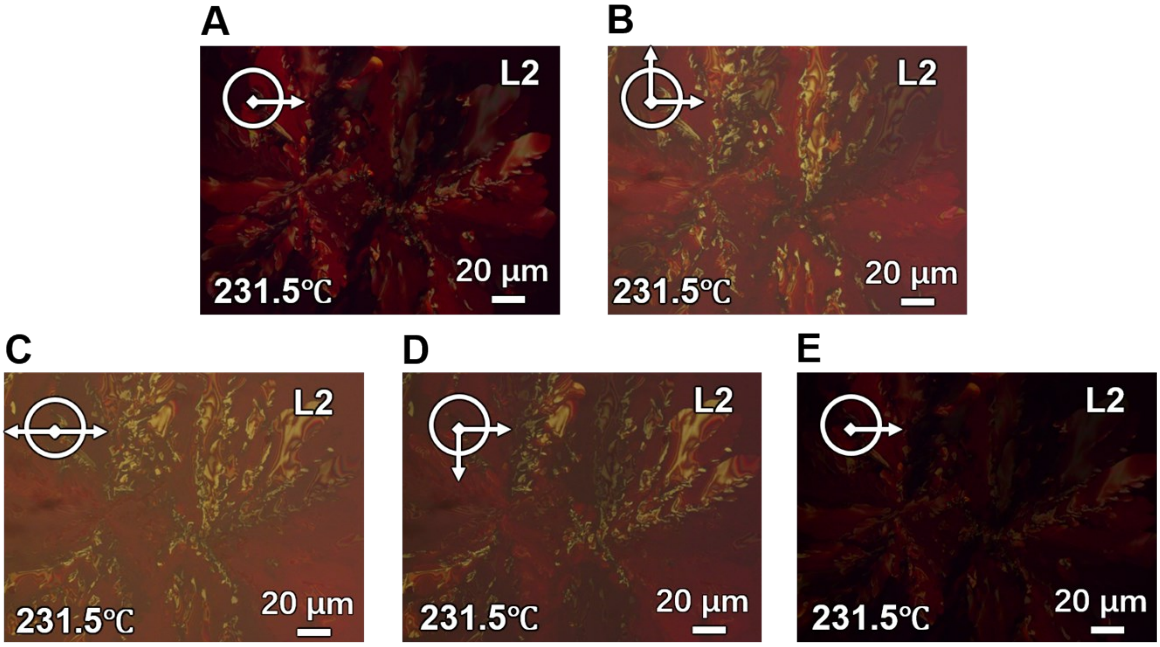

Figure S11. POM images of L2 neat film taken at different polarizer and the analyzer angles.

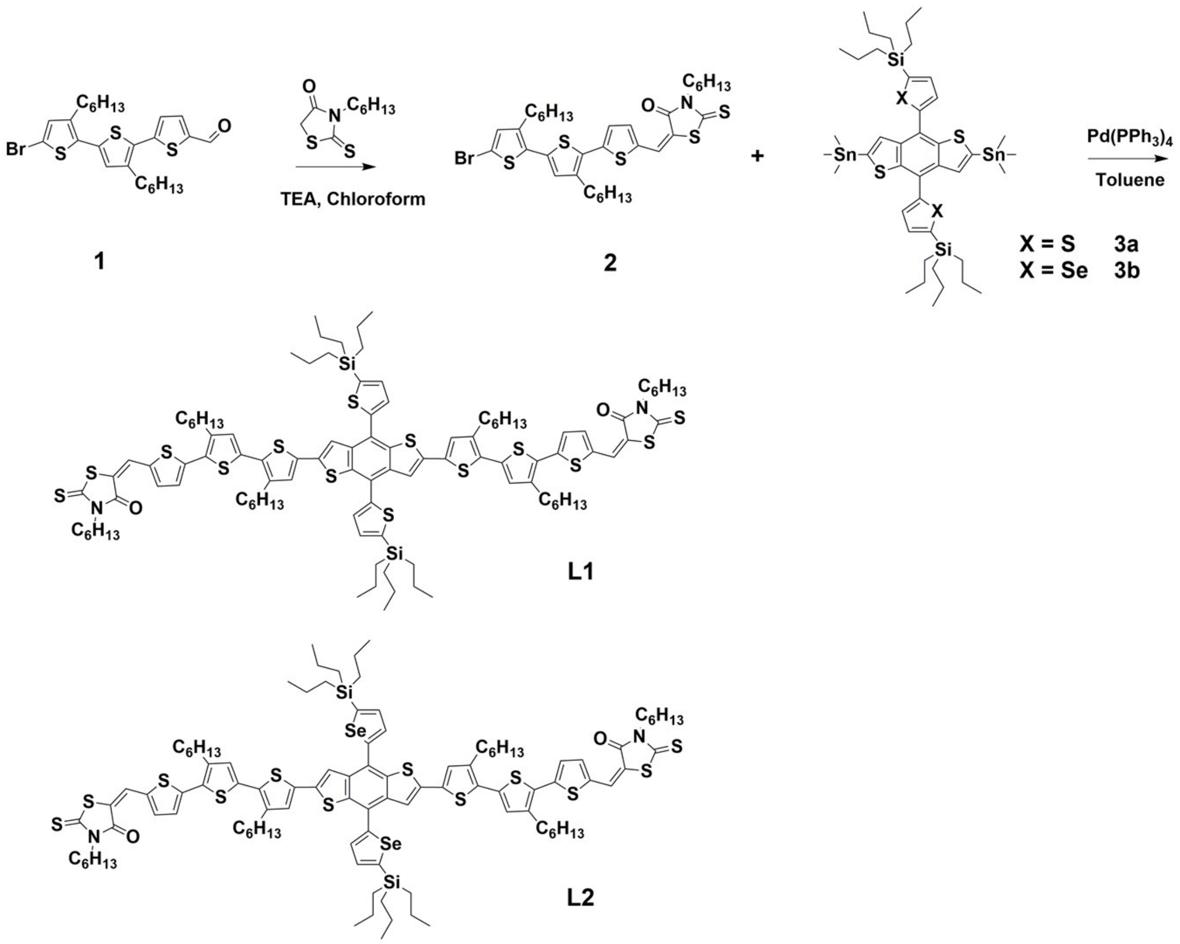

Figure S12. Synthetic route of L1 and L2.

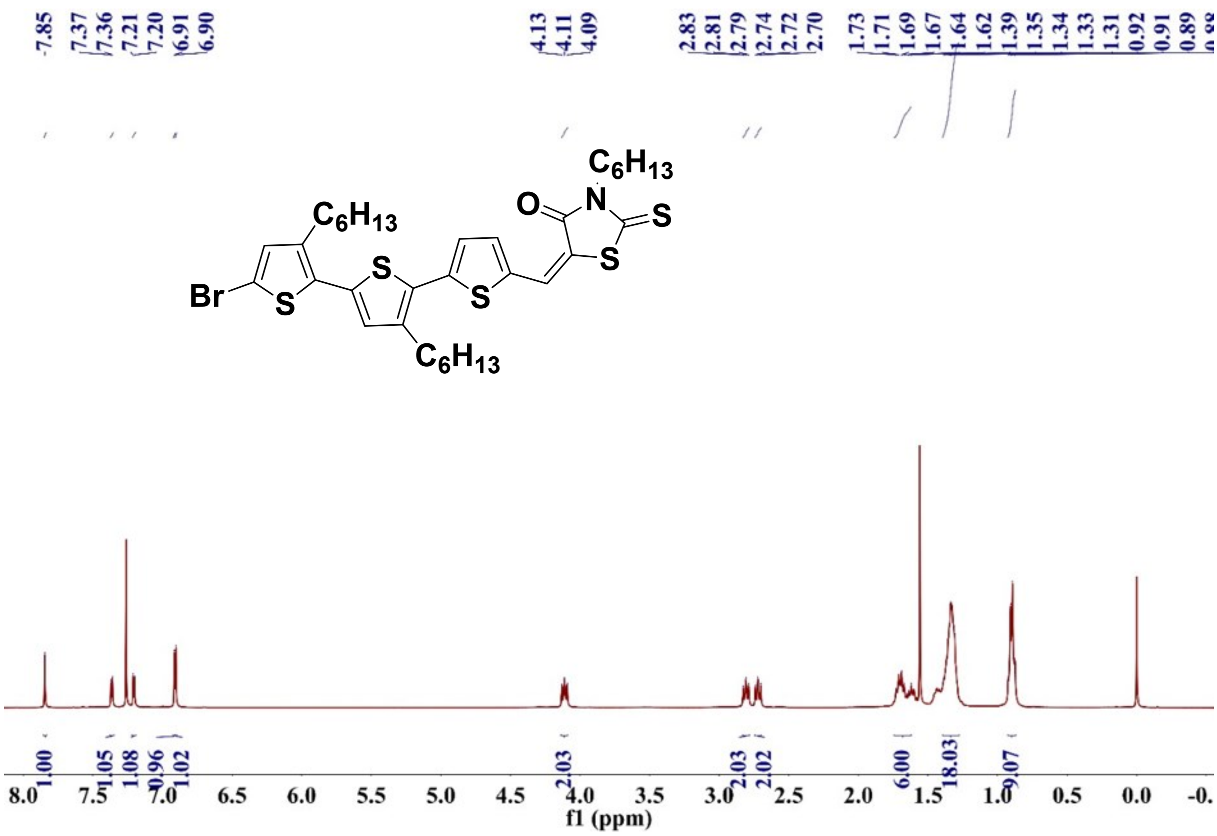

Figure S13. ^{1}H NMR spectrum of compound 3 in $CDCl_3$.

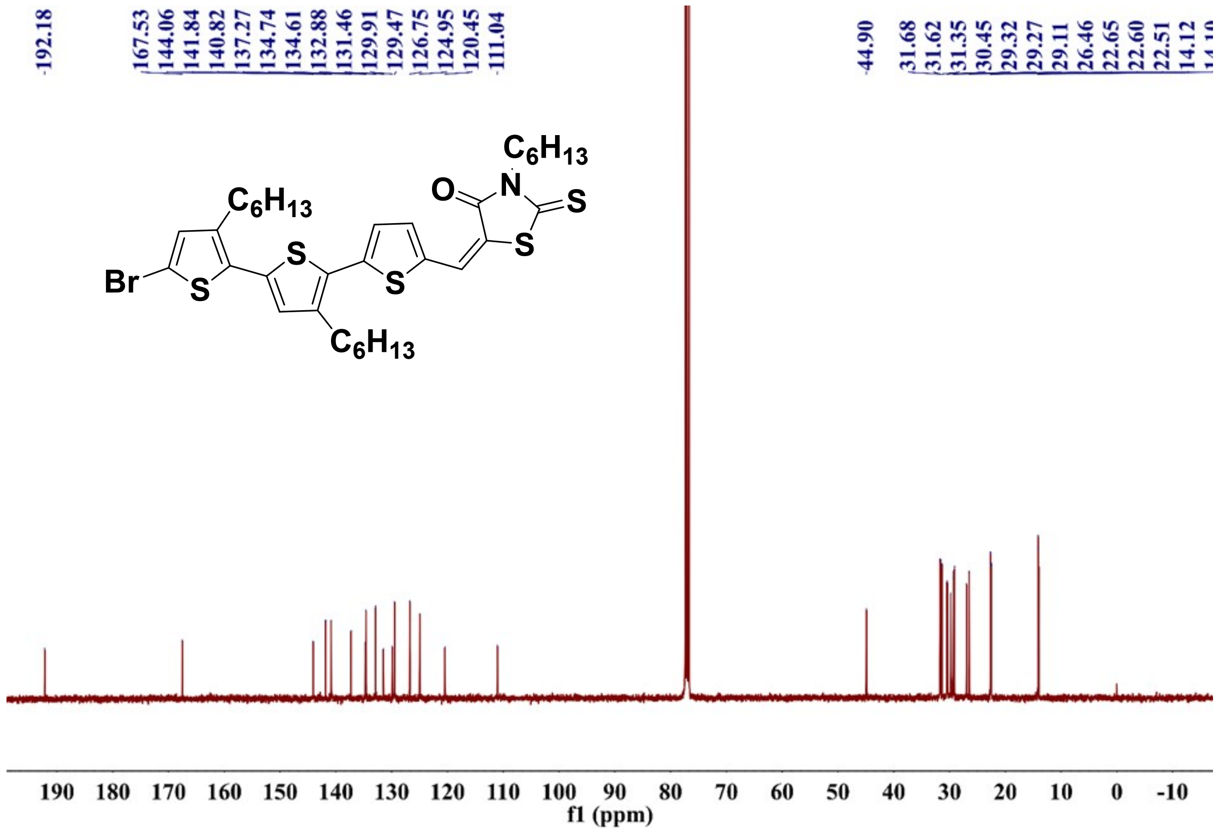

Figure S14. ^{13}C NMR spectrum of **2** in $CDCl_3$.

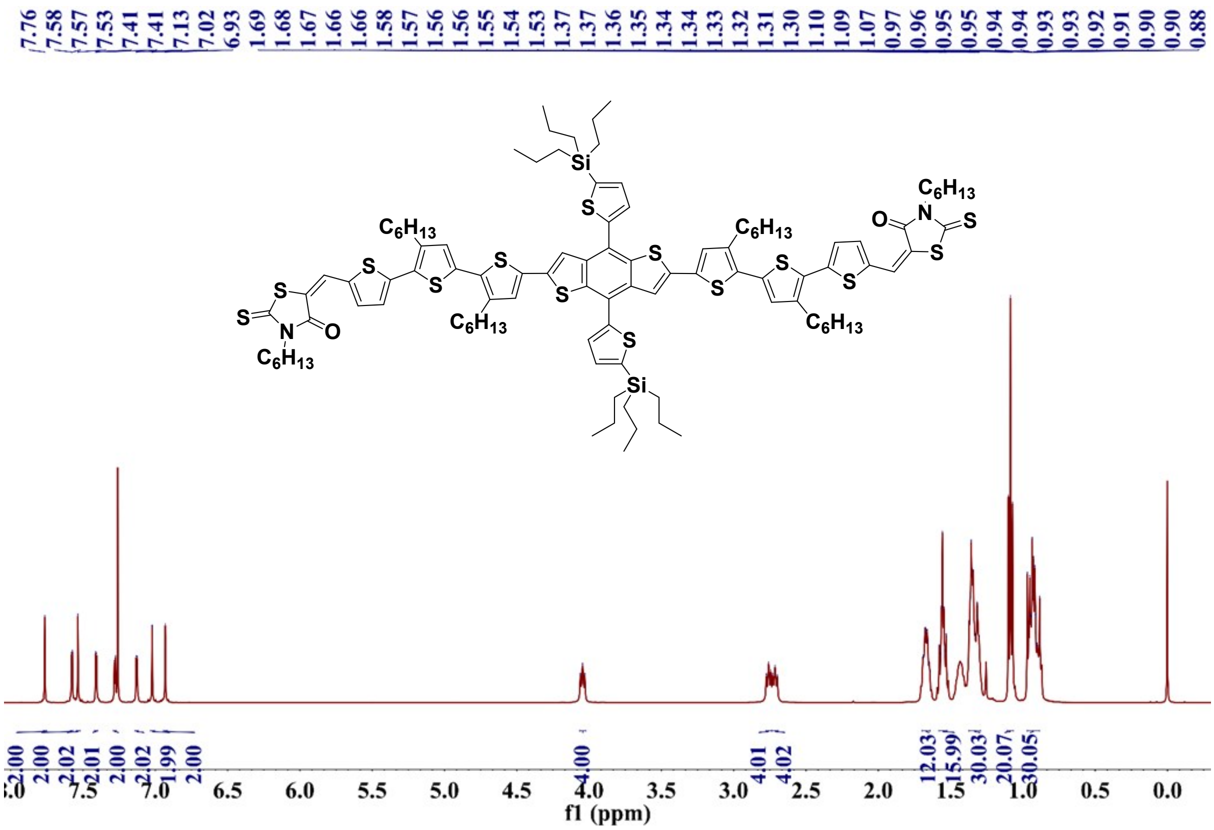

Figure S15. ^{1}H NMR spectrum of **L1** in $CDCl_3$.

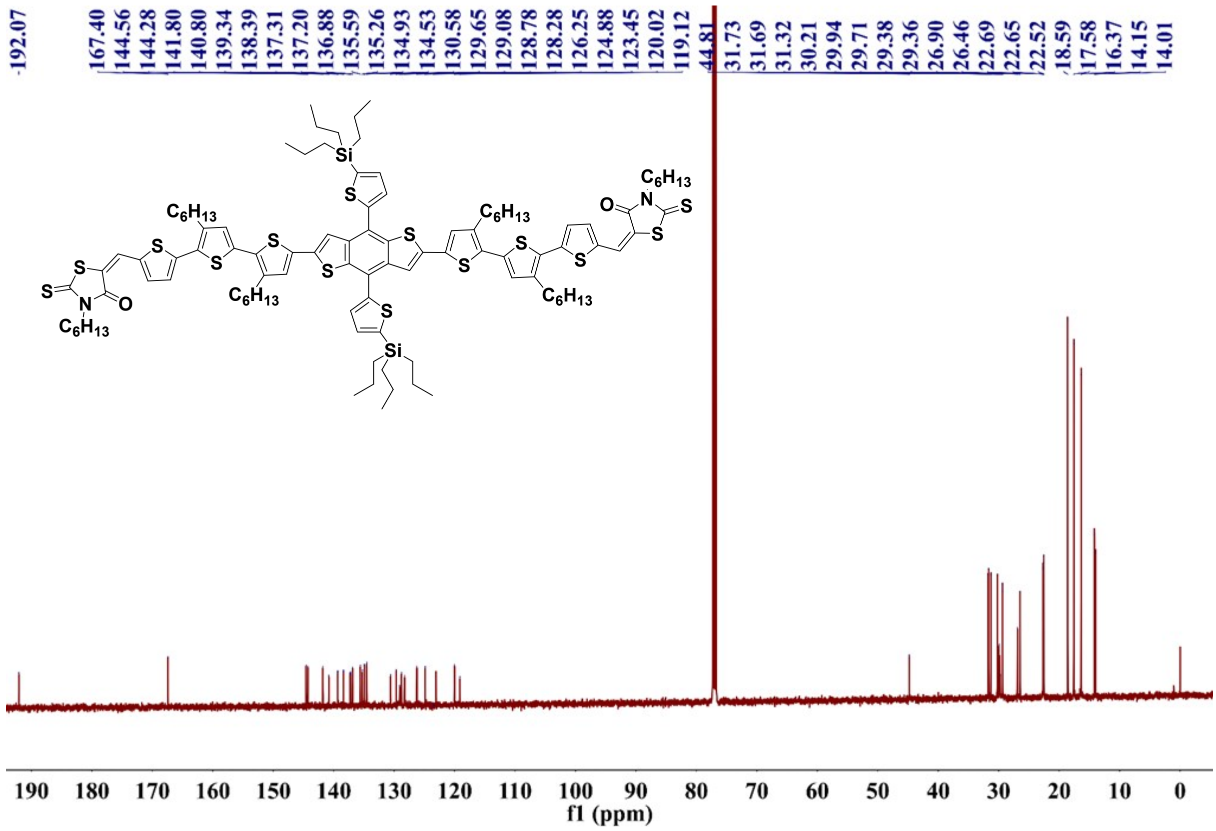

Figure S16. ^{13}C NMR spectrum of **L1** in $CDCl_3$.

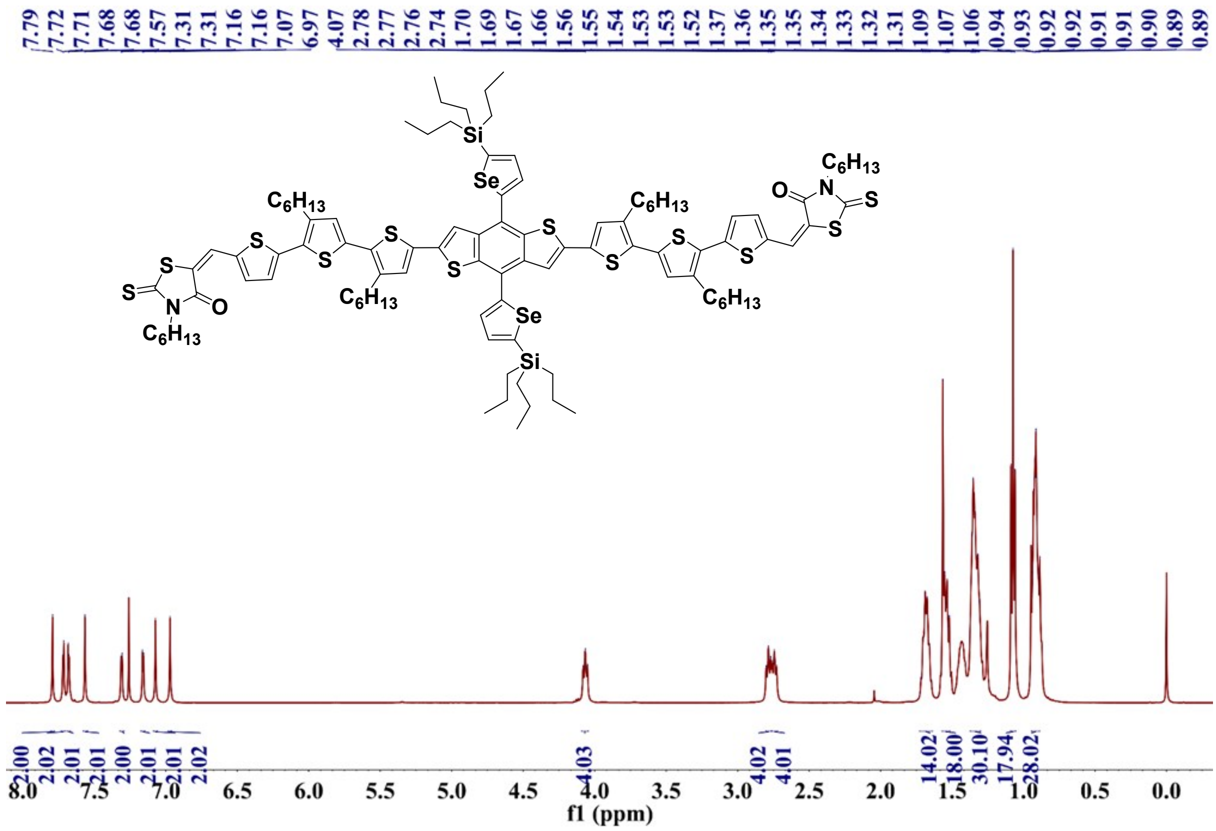

Figure S17. ^{1}H NMR spectrum of **L2** in $CDCl_3$.

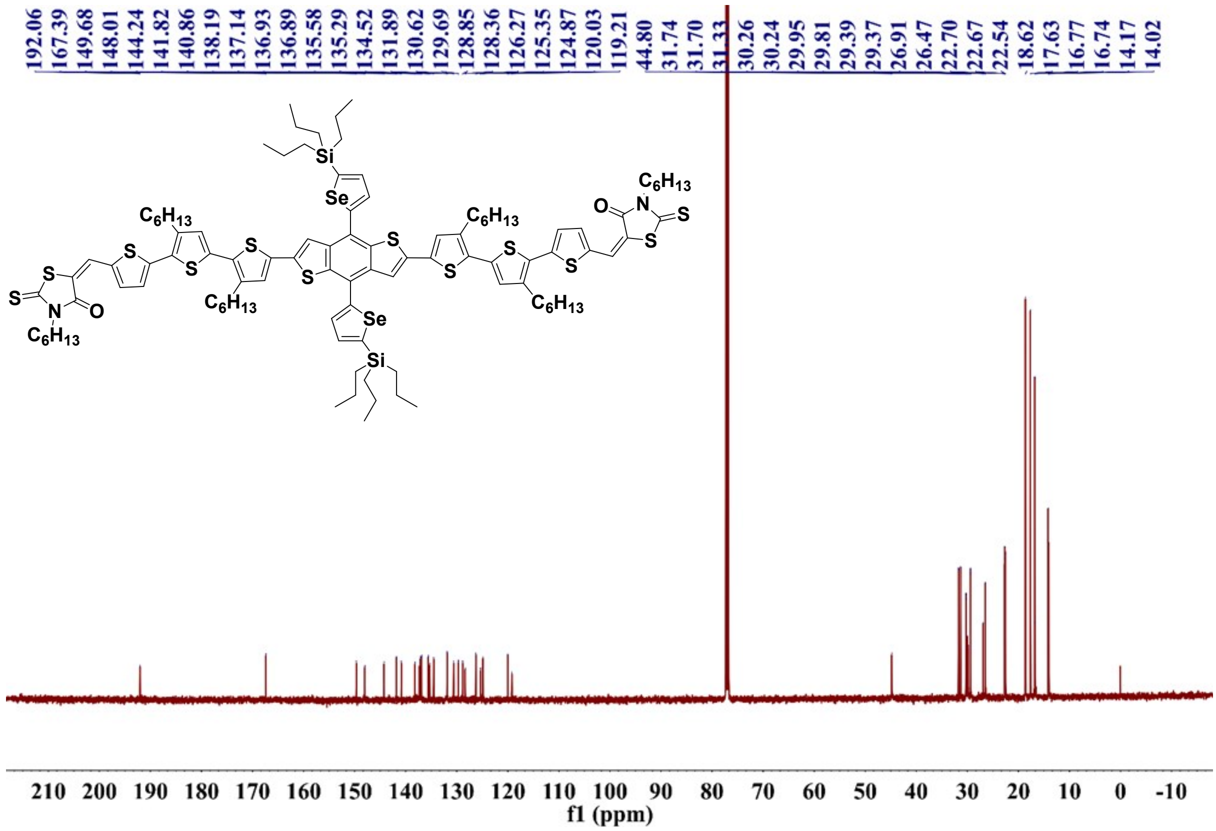

Figure S18. ^{13}C NMR spectrum of **L2** in $CDCl_3$.

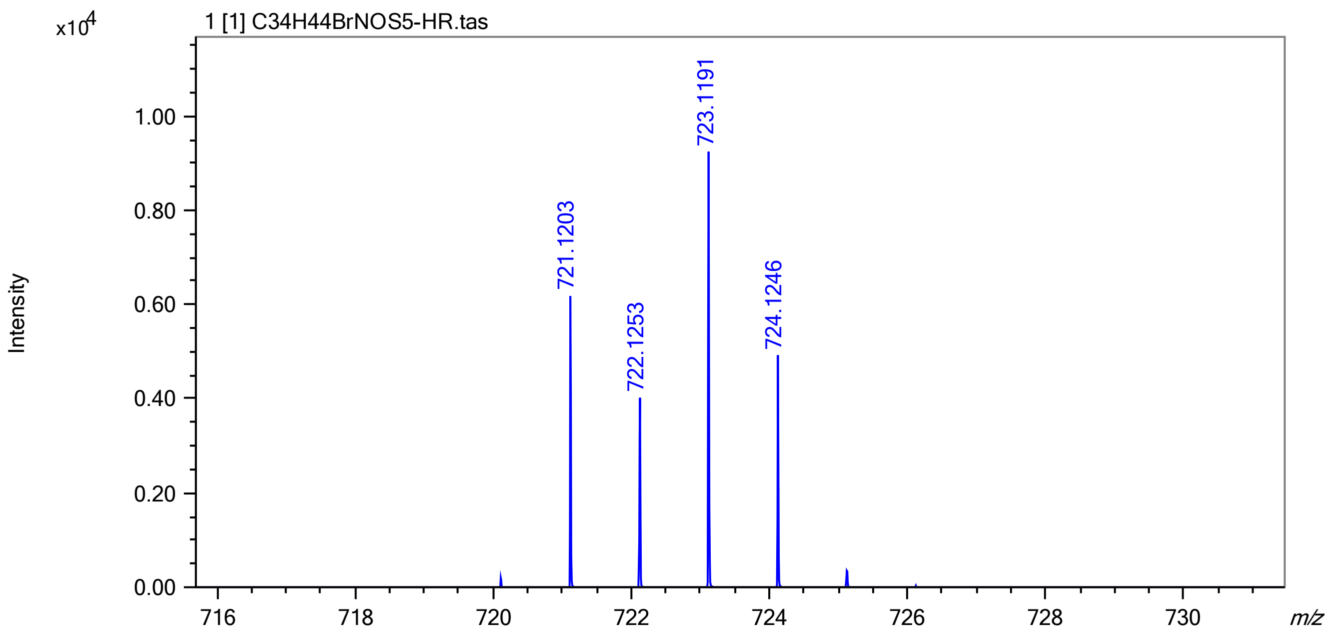

Figure S19. MALDI-TOF MS of compound **2.**

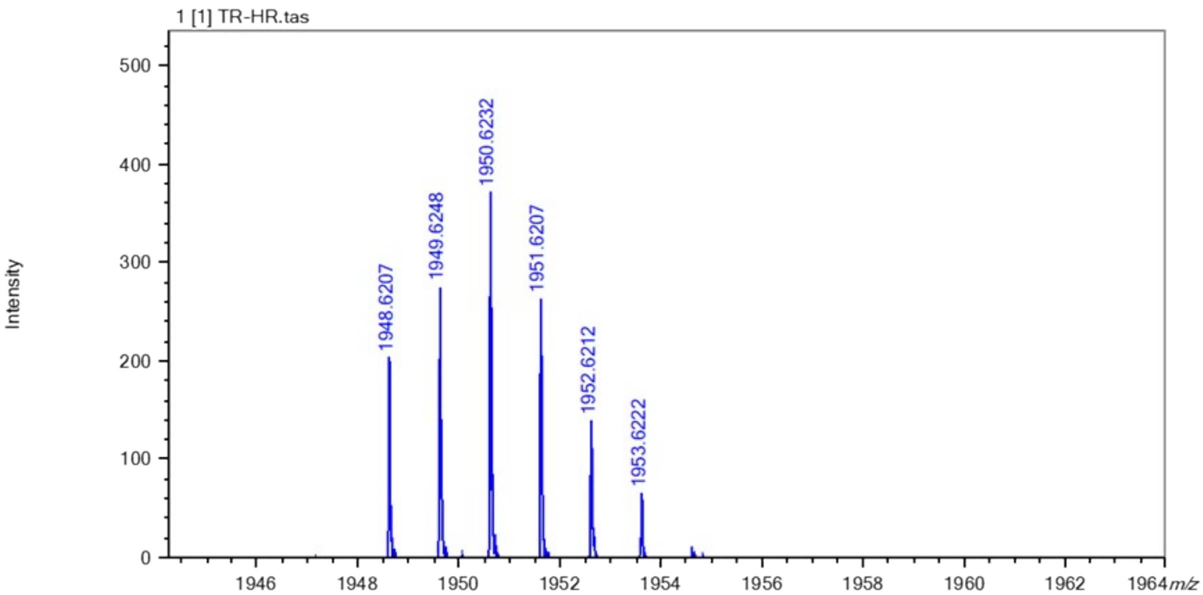

Figure S20. MALDI-TOF MS of **L1.**

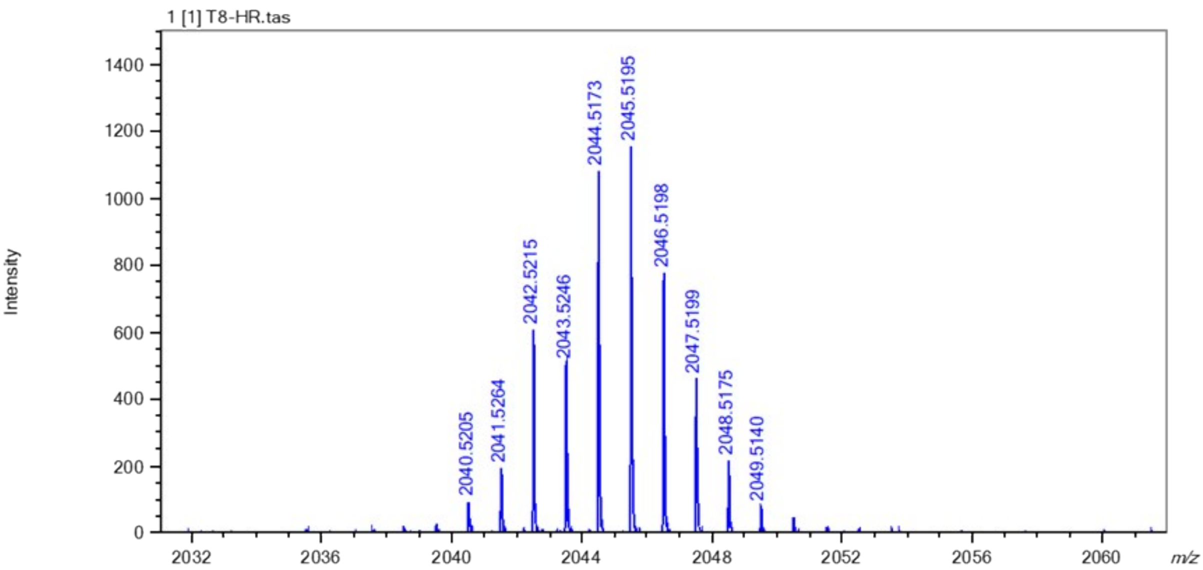

Figure S21. MALDI-TOF MS of **L2.**

Supplementary Tables

Table S1. The exciton dissociation efficiency ($\eta_{diss} = J_{ph,SC}/J_{ph,sat}$) and charge collection efficiency ($\eta_{coll} = J_{ph,max\ power}/J_{ph,sat}$) of L1:Y6 and L2:Y6 devices.

Parameter	L1:Y6	L2:Y6
$J_{ph,\ sat}$ (mA cm^{-2})	26.55	26.95
$J_{ph,\ SC}$ (mA cm^{-2})	25.28	26.35
$\eta_{diss} = J_{ph,\ SC}/J_{ph,\ sat}$ (%)	95.20	97.80
$J_{ph,\ max}$ (mA cm^{-2})	21.23	22.50
$\eta_{coll} = J_{ph,\ max\ power}/J_{ph,\ sat}$ (%)	79.96	83.49

Table S2. Photovoltaic data for high-efficiency binary-OSCs (PCE > 10%) reported in recent 6 years.

Donor	Acceptor	V_{OC}[V]	PCE[%]	FF [%]	J_{SC} [mA cm^{-2}]	Ref.
DRCN5T	$PC_{71}BM$	0.92	10.08	69.0	15.88	1
BTID-2F	$PC_{71}BM$	0.95	11.30	76.0	15.70	2
BDTTS-Cl-R	$PC_{71}BM$	0.96	10.78	75.3	14.92	3
DRTB-T-C4	IT-4F	0.91	11.24	68.0	18.27	4
ZnP-TBO	6TIC	0.80	12.08	73.87	20.44	5
BTR-Cl	Y6	0.86	13.60	66.0	24.17	6
ZR1	Y6	0.861	14.34	68.44	24.34	7
B1	BO-4Cl	0.83	15.3	73.0	25.27	8
L2	Y6	0.83	15.8	72.1	26.35	**This Work**

Table S3. Photovoltaic data for high-efficiency thickness ASM OSCs (PCE > 9%) reported in recent 6 years.

Active layer	Thickness [nm]	V_{OC} [V]	PCE[%]	FF [%]	J_{SC} [mA cm^{-2}]	Ref.
DR3TSBDT:$PC_{71}BM$	280	0.88	9.05	65.3	15.82	[9]
BTR:$PC_{71}BM$	310	0.94	9.50	70.0	14.50	[10]
DRTB-T-C4: IT-4F	300	0.893	10.18	61.0	18.68	[4]
BTR:NITI:$PC_{71}BM$	300	0.94	13.63	73.83	19.50	[11]
BTR:BTR-OH:$PC_{71}BM$	300	0.93	10.14	74.2	14.62	[12]
SM1-F:Y6	250	0.85	11.9	64.0	21.90	[13]
L1:Y6	300	0.81	13.8	70.5	24.31	**This Work**
L2:Y6	300	0.82	14.3	71.2	24.50	

Table S4. Photovoltaic data of L1:Y6 solar cells with different time of CS_2 solvent annealing. All data were obtained under illumination of AM 1.5G (100mW cm^{-2}) light source.

Materials	Condition	V_{OC} [V]	J_{SC} [mA cm^{-2}]	FF [%]	[a] PCE [%]
L1:Y6 1.5:1	CS_2,15s	0.83 (0.84±0.01)	24.12 (24.09±0.02)	68.6 (67.3±1.3)	13.8 (13.6±0.2)
	CS_2,20s	0.84 (0.83±0.01)	23.81 (24.09±0.28)	69.6 (66.8±2.8)	13.9 (13.4±0.5)
	CS_2,25s	0.84 (0.84±0.01)	23.67 (23.53±0.14)	67.7 (66.4±1.3)	13.6 (13.2±0.4)
	CS_2,30s	0.83 (0.83±0.01)	23.68 (23.63±0.05)	68.3 (66.3±2.1)	13.5 (13.0±0.5)

[a] The average parameters were calculated over 10 independent cells.

Table S5. Photovoltaic data of L1:Y6 solar cells with thermal annealed at different times after CS_2 solvent annealing for the same time. All data were obtained under illumination of AM 1.5G (100mW cm^{-2}) light source.

Materials	Condition	V_{OC} [V]	J_{SC} [mA cm^{-2}]	FF [%]	[a] PCE [%]
L1:Y6 1.5:1	CS_2,15s	0.83 (0.84±0.01)	24.12 (24.09±0.02)	68.6 (67.3±1.3)	13.8 (13.6±0.2)
	CS_2,15s, 110℃,2min	0.83 (0.83±0.01)	24.15 (24.25±0.10)	67.3 (66.2±1.1)	13.5 (13.3±0.2)
	CS_2,15s, 110℃,5min	0.83 (0.82±0.01)	23.72 (23.61±0.11)	66.5 (65.9±0.5)	13.1 (12.8±0.3)

[a] The average parameters were calculated over 10 independent cells.

Table S6. The photovoltaic data of L1:Y6 solar cells with different donor/acceptor ratios. All data were obtained under illumination of AM 1.5G (100mW cm^{-2}) light source.

D:A ratio	Condition	V_{OC} [V]	J_{SC} [mA cm^{-2}]	FF [%]	[a]PCE [%]
1.2:1	CS_2,20s	0.82 (0.81±0.01)	24.77 (24.42±0.35)	62.5 (60.5±1.9)	12.7 (12.1±0.7)
1.3:1	CS_2,20s	0.82 (0.82±0.01)	23.72 (23.75±0.03)	66.1 (62.3±3.8)	12.9 (12.2±0.7)
1.5:1	CS_2,20s	0.84 (0.83±0.01)	23.81 (24.09±0.28)	69.6 (66.8±2.8)	13.9 (13.4±0.5)
1.7:1	CS_2,20s	0.81 (0.81±0.01)	24.02 (23.74±0.27)	67.3 (65.8±1.5)	13.2 (12.8±0.4)

[a] The average parameters were calculated over 10 independent cells.

Table S7. Photovoltaic data of L1:Y6 solar cells with thermal annealed at the same times after CS_2 solvent annealing for different times. All data were obtained under illumination of AM 1.5G (100mW cm^{-2}) light source.

Materials	Condition	V_{OC} [V]	J_{SC} [mA cm^{-2}]	FF [%]	[a]PCE [%]
L1:Y6 1.5:1	CS_2,20s,110℃,2min	0.83 (0.83±0.01)	25.75 (25.38±0.37)	67.2 (66.8±0.4)	14.2 (14.0±0.3)
	CS_2,30s,110℃,2min	0.83 (0.83±0.01)	25.24 (25.11±0.12)	68.8 (67.7±1.1)	14.4 (14.1±0.3)
	CS_2,40s,110℃,2min	0.83 (0.82±0.01)	25.28 (25.18±0.10)	69.8 (68.3±1.5)	14.6 (14.2±0.4)
	CS_2,50s,110℃,2min	0.83 (0.82±0.01)	25.13 (25.01±0.12)	68.9 (68.3±0.6)	14.3 (14.1±0.2)
	CS_2,60s,110℃,2min	0.83 (0.82±0.01)	24.86 (25.03±0.17)	67.6 (66.1±1.5)	14.0 (13.6±0.4)

a) The average PCE values were obtained from 15 devices.

Table S8. The photovoltaic data of the L2:Y6 solar cells with thermal annealed at different temperature after CS_2 solvent annealing for the same time. All data were obtained under illumination of AM 1.5G (100mW cm^{-2}) light source.

Materials	Condition	V_{OC} [V]	J_{SC} [mA cm^{-2}]	FF [%]	[a] PCE [%]
L2:Y6 1.5:1	100℃,10min, CS_2,30s	0.83 (0.83±0.01)	23.2 (23.1±0.1)	70.6 (68.6±2.0)	13.53 (13.20±0.33)
	105℃,10min, CS_2,30s	0.82 (0.82±0.01)	22.5 (22.4±0.1)	73.1 (72.1±1.0)	13.49 (13.30±0.19)
	110℃,10min, CS_2,30s	0.79 (0.81±0.02)	23.7 (23.6±0.1)	74.9 (71.3±3.6)	14.02 (13.60±0.41)
	120℃,10min, CS_2,30s	0.81 (0.80±0.01)	23.7 (23.6±0.1)	71.3 (69.9±1.4)	13.64 (13.29±0.35)
	130℃,10min, CS_2,30s	0.83 (0.81±0.02)	23.7 (23.5±0.2)	64.4 (63.0±1.4)	12.69 (12.02±0.67)
	140℃,10min, CS_2,30s	0.80 (0.79±0.01)	23.8 (23.9±0.1)	64.5 (60.0±4.5)	12.28 (11.37±0.92)

[a] The average PCE values were obtained from 10 devices.

Table S9. The photovoltaic data of the L2:Y6 solar cells with different ratios. All data were obtained under illumination of AM 1.5G (100mW cm^{-2}) light source.

D:A ratio	Condition	V_{OC} [V]	J_{SC} [mA cm-2]	FF [%]	[a] PCE [%]
1.4:1	110°C,10min, CS_2,30s	0.82 (0.82±0.01)	22.8 (23.6±0.2)	66.9 (61.7±5.2)	12.53 (11.91±0.62)
1.5:1	110°C,10min, CS_2,30s	0.81 (0.80±0.01)	23.7 (23.6±0.1)	71.3 (69.9±1.4)	13.64 (13.29±0.35)
1.6:1	110°C,10min, CS_2,30s	0.82 (0.81±0.01)	23.5 (23.4±0.1)	63.5 (62.1±1.4)	12.31 (11.84±0.47)

[a] The average PCE values were obtained from 10 devices.

Table S10. The photovoltaic data of L2:Y6 solar cells with thermal annealed at different times after CS_2 solvent annealing for the same time. All data were obtained under illumination of AM 1.5G (100mW cm^{-2}) light source.

Materials	Condition	V_{OC} [V]	J_{SC} [mA cm^{-2}]	FF [%]	[a] PCE [%]
L2:Y6 1.5:1	CS_2,30s,110°C,1min	0.82 (0.82±0.01)	25.31 (25.10±0.21)	70.9 (70.3±0.6)	14.8 (14.5±0.3)
	CS_2,30s,110°C,2min	0.82 (0.82±0.01)	25.78 (25.01±0.77)	69.8 (70.1±0.2)	14.9 (14.5±0.4)
	CS_2,30s,110°C,5min	0.82 (0.82±0.01)	25.15 (25.13±0.02)	71.4 (69.7±1.7)	14.7 (14.4±0.4)
	CS_2,30s,110°C,10min	0.82 (0.82±0.01)	24.94 (24.44±0.50)	69.7 (69.4±0.3)	14.3 (13.9±0.4)

[a] The average PCE values were obtained from 10 devices.

Table S11. Photovoltaic data of L2:Y6 solar cells with thermal annealed at the same times after CS_2 solvent annealing for different times. All data were obtained under illumination of AM 1.5G (100mW cm^{-2}) light source.

Materials	Condition	V_{OC} [V]	J_{SC} [mA cm^{-2}]	FF [%]	[a] PCE [%]
L2:Y6 1.5:1	CS_2,20s,110℃,2min	0.84 (0.84±0.01)	25.65 (25.30±0.35)	68.0 (67.9±0.1)	14.6 (14.4±0.2)
	CS_2,30s,110℃,2min	0.82 (0.82±0.01)	25.78 (25.01±0.77)	69.8 (70.1±0.2)	14.9 (14.5±0.4)
	CS_2,40s,110℃,2min	0.83 (0.82±0.01)	25.77 (25.59±0.18)	72.8 (72.4±0.4)	15.5 (15.3±0.3)
	CS_2,50s,110℃,2min	0.82 (0.81±0.01)	26.13 (26.25±0.12)	70.4 (68.0±2.4)	15.1 (14.6±0.3)
	CS_2,60s,110℃,2min	0.83 (0.82±0.01)	26.60 (26.59±0.10)	67.8 (65.7±2.2)	14.9 (14.4±0.4)

[a] The average PCE values were obtained from 10 devices.

Table S12. The photovoltaic data of L2:Y6 solar cells with thermal annealed at different times after CS_2 solvent annealing for the same time. All data were obtained under illumination of AM 1.5G (100mW cm^{-2}) light source.

Materials	Condition	V_{OC} [V]	J_{SC} [mA cm^{-2}]	FF [%]	[a] PCE [%]
L2:Y6 1.5:1	CS_2,40s,80℃,2min	0.84 (0.84±0.01)	25.31 (25.17±0.13)	69.0 (67.3±1.7)	14.7 (14.2±0.5)
	CS_2,40s,90℃,2min	0.83 (0.83±0.01)	25.57 (25.36±0.21)	72.3 (72.2±0.1)	15.4 (15.2±0.2)
	CS_2,40s,110℃,2min	0.83 (0.82±0.01)	26.35 (26.24±0.11)	72.1 (70.4±1.6)	15.8 (15.4±0.4)
	CS_2,40s,120℃,2min	0.83 (0.82±0.01)	25.39 (25.33±0.06)	70.8 (68.4±2.4)	14.8 (14.3±0.5)

[a] The average PCE values were obtained from 10 devices.

Table S13. The photovoltaic data of the L2:Y6 solar cells with different ratios. All data were obtained under illumination of AM 1.5G (100mW cm^{-2}) light source.

D:A ratio	Condition	V_{OC} [V]	J_{SC} [mA cm^{-2}]	FF [%]	[a] PCE [%]
1.4:1	CS_2,40s,90℃,2min	0.82 (0.83±0.01)	25.02 (25.01±0.01)	66.8 (66.6±0.2)	13.9 (13.8±0.1)
1.5:1	CS_2,40s,90℃,2min	0.83 (0.83±0.01)	25.57 (25.36±0.21)	72.3 (72.2±0.1)	15.4 (15.2±0.2)
1.6:1	CS_2,40s,90℃,2min	0.83 (0.83±0.01)	25.25 (25.01±0.24)	71.4 (70.4±1.0)	15.1 (14.6±0.5)

[a] The average PCE values were obtained from 10 devices.

Table S14. Detailed GIWAXS (100) peak information IP and OOP of L1:Y6 and L2:Y6 blend film.

[a]Component	Peak	Peak location ($Å^{-1}$)	FWHM (Å−1)	Crystal coherence length(nm)
L1:Y6 As Cast	(100) IP	0.309	0.091	62.14
	(010) OOP	1.68	0.213	26.55
L1:Y6, CS_2 40s, TA 2min	(100) IP	0.326	0.039	145.00
	(100) OOP	0.323	0.062	91.21
	(200) OOP	0.647	0.068	83.16
	(010) OOP	1.683	0.194	29.15
L2:Y6 As Cast	(100) IP	0.301	0.085	66.53
	(010) OOP	1.68	0.208	27.19
L2:Y6, CS_2 40s, TA 2min	(100) IP	0.303	0.032	176.71
	(100) OOP	0.313	0.038	148.81
	(200) OOP	0.645	0.056	100.98
	(010) OOP	1.689	0.159	35.57

[a]TA: 110℃.

Table S15. Detailed GIWAXS (100) peak information IP and OOP of L1 and L2 neat film.

Component	Peak	Peak location (Å−1)	FWHM (Å−1)	Crystal coherence length(nm)
L1	(100) OOP	0.323	0.063	89.76
	(200) OOP	0.665	0.05	113.10
	(300) OOP	0.998	0.068	83.16
	(100) IP	0.325	0.039	145.00
	(010) IP	1.666	0.15	37.70
L2	(100) OOP	0.312	0.078	72.50
	(200) OOP	0.646	0.044	128.52
	(300) OOP	0.973	0.066	85.68
	(100) IP	0.319	0.036	157.08
	(010) IP	1.674	0.147	38.47

Table S16. Dark J–V curves of the OSCs: a) electron-only diodes and hole-only; The solid lines are fit to the experimental data according to the equation 2.

Active layer	μ_h [$\times 10^{-4}$ cm^2 V^{-1} s^{-1}]	μ_e [$\times 10^{-3}$ cm^2 V^{-1} s^{-1}]	μ_h / μ_e
L1:Y6	6.43±2.51	1.29±1.44	0.50
L2:Y6	7.72±1.83	1.51±1.08	0.51

References

1. B. Kan *et al.*, A Series of Simple Oligomer-like Small Molecules Based on Oligothiophenes for Solution-Processed Solar Cells with High Efficiency. *J. Am. Chem. Soc.*, **137**, 3886-3893 (2015).
2. D. Deng *et al.*, Fluorination-enabled optimal morphology leads to over 11% efficiency for inverted small-molecule organic solar cells. *Nat. Commun.*, **7**, 13740 (2016).
3. Z. Ji, X. Xu, G. Zhang, Y. Li and Q. Peng, Synergistic effect of halogenation on molecular energy level and photovoltaic performance modulations of highly efficient small molecular materials. *Nano. Energy.*, **40**, 214-223 (2017).
4. L. Yang *et al.*, Modulating Molecular Orientation Enables Efficient Nonfullerene Small-Molecule Organic Solar Cells. *Chem. Mater.*, **30**, 2129-2134 (2018).
5. K. Gao *et al.*, Over 12% Efficiency Nonfullerene All-Small-Molecule Organic Solar Cells with Sequentially Evolved Multilength Scale Morphologies. *Adv. Mater.*, **31**, 1807842 (2019).
6. H. Chen *et al.*, All-Small-Molecule Organic Solar Cells with an Ordered Liquid Crystalline Donor. *Joule*, **3**, 3034-3047 (2019).
7. R. Zhou *et al.*, All-small-molecule organic solar cells with over 14% efficiency by optimizing hierarchical morphologies. *Nat. Commun.*, **10**, 5393 (2019).
8. J. Qin *et al.*, 15.3% efficiency all-small-molecule organic solar cells enabled by symmetric phenyl substitution. *Science China Materials*, **63**, 1142-1150 (2020).
9. Q. Zhang *et al.*, Large active layer thickness toleration of high-efficiency small molecule solar cells. *J. Mater. Chem. A*, **3**, 22274-22279 (2015).
10. A. Armin *et al.*, Reduced Recombination in High Efficiency Molecular Nematic Liquid Crystalline: Fullerene Solar Cells. *Adv. Energy Mater.*, **6**, 1600939 (2016).
11. Z. Zhou *et al.*, High-efficiency small-molecule ternary solar cells with a hierarchical morphology enabled by synergizing fullerene and non-fullerene acceptors. *Nature Energy*, **3**, 952-959 (2018).
12. H. Tang *et al.*, Donor Derivative Incorporation: An Effective Strategy toward High Performance All-Small-Molecule Ternary Organic Solar Cells. *Adv Sci (Weinh)*, **6**, 1901613 (2019).
13. B. Qiu *et al.*, Highly Efficient All-Small-Molecule Organic Solar Cells with Appropriate Active Layer Morphology by Side Chain Engineering of Donor Molecules and Thermal Annealing. *Adv. Mater.*, **32**, 1908373 (2020).